THE JOURNAL OF BIOLOGICAL CHEMISTRY
Vol. 276, No. 46, Issue of November 16, pp. 42965–42970, 2001

Printed in U.S.A.

Apolipoprotein A-I Adopts a Belt-like Orientation in Reconstituted High Density Lipoproteins*

Received for publication, July 10, 2001, and in revised form, September 12, 2001
Published, JBC Papers in Press, September 13, 2001, DOI 10.1074/jbc.M106462200

Stacey E. Panagotopulos, Erica M. Horace, J. Nicholas Maiorano, and W. Sean Davidson‡

From the Department of Pathology and Laboratory Medicine, University of Cincinnati, Cincinnati, Ohio 45267-0529

Apolipoprotein A-I (apoA-I) is the major protein associated with high density lipoprotein (HDL), and its plasma levels have been correlated with protection against atherosclerosis. Unfortunately, the structural basis of this phenomenon is not fully understood. Over 25 years of study have produced two general models of apoA-I structure in discoidal HDL complexes. The "belt" model states that the amphipathic helices of apoA-I are aligned perpendicular to the acyl chains of the lipid bilayer, whereas the "picket fence" model argues that the helices are aligned parallel with the acyl chains. To distinguish between the two models, various single tryptophan mutants of apoA-I were analyzed in reconstituted, discoidal HDL particles composed of phospholipids containing nitroxide spin labels at various positions along the acyl chain. We have previously used this technique to show that the orientation of helix 4 of apoA-I is most consistent with the belt model. In this study, we performed additional control experiments on helix 4, and we extended the results by performing the same analysis on the remaining 22-mer helices (helices 1, 2, 5, 6, 7, 8, and 10) of human apoA-I. For each helix, two different mutants were produced that each contained a probe Trp occurring two helical turns apart. In the belt model, the two Trp residues in each helix should exhibit maximal quenching at the same nitroxide group position on the lipid acyl chains. For the picket fence model, maximal quenching should occur at two different levels in the bilayer. The results show that the majority of the helices are in an orientation that is consistent with a belt model, because most Trp residues localized to a position about 5 Å from the center of the bilayer. This study corroborates a belt hypothesis for the majority of the helices of apoA-I in phospholipid discs.

Because of sedentary lifestyles and high fat diets, atherosclerosis remains one of the leading causes of death in the Western world. It has been demonstrated repeatedly that levels of high density lipoprotein (HDL)[1] and its major protein constituent apolipoprotein A-I (apoA-I) are inversely correlated with the incidence of heart disease (1). Apo-AI, a 28-kDa protein made up of 11- and 22-mer amphipathic helices (Ref. 2; reviewed in Ref. 3), is critical to the formation and stability of the HDL particle in circulation. The process of reverse cholesterol transport is thought to remove excess cholesterol from extra-hepatic tissues such as the arterial wall and return it to the liver for processing (4, 5). ApoA-I performs many critical functions in this pathway. In the lipid poor form, it can interact with the cell surface under the control of the ATP-binding cassette A1 transporter (6). Once apoA-I accumulates phospholipids and cholesterol from the cell surface, it likely forms discoidal complexes that interact with enzymes such as lecithin:cholesterol acetyl transferase and cholesterol ester transfer protein to form the spherical HDL particles commonly found in plasma. These are the particles that are thought to deliver cholesterol to the liver and steroidogenic tissues through interaction with scavenger receptor type B class I (7).

ApoA-I has a dynamic structure that allows it to perform its functions. Numerous attempts have been made to determine the arrangement of the amphipathic helices in nascent HDL discs, because this appears to be a critical intermediate in reverse cholesterol transport. Early studies including primary sequence analyses (8), dried film infrared spectroscopy (9, 10), and particle geometry calculations (11) were interpreted to be in support of a "picket fence" model in which the helices of apoA-I are arranged parallel to the phospholipid bilayer. Recent computer simulation studies have also supported this model (12).

However, other computer models derived from a crystal structure of a lipid free fragment of apoA-I suggest the possibility of a "belt" model (13, 14). In this case, the helices of apoA-I are arranged perpendicular to the phospholipid bilayer. Further support for this model comes from a recent study that employed oriented polarized internal reflection infrared spectroscopy (15) to show that, on average, most of the helical regions are consistent with a belt orientation in phospholipid discs.

Using a new approach that capitalized on the fluorescence of introduced tryptophan residues and the quenching ability of nitroxide spin-labeled phospholipids, our laboratory experimentally determined the orientation of helix 4 in apoA-I (16). Two different positions were chosen in the helix, one at the center (residue 108) and one near the C-terminal end of the helix (residue 115), for making single Trp mutants of apoA-I. Nitroxide labels on phospholipid acyl chains were placed at five different depths in separate reconstituted HDL (rHDL) particles containing each of these mutants. The depth of each Trp was determined by a modification of the parallax analysis commonly used to study membrane spanning proteins (17). In the belt model, the Trp residues in both mutants would be maximally quenched at the same level in the bilayer; in the picket fence model the Trp residues would be quenched at

* This work was supported in part by Grant RO1 HL62542 from the NHLBI, National Institutes of Health (to W. S. D.). The costs of publication of this article were defrayed in part by the payment of page charges. This article must therefore be hereby marked "*advertisement*" in accordance with 18 U.S.C. Section 1734 solely to indicate this fact.

‡ Established Investigator of the American Heart Association. To whom correspondence should be addressed: Dept. of Pathology and Laboratory Medicine, University of Cincinnati, 231 Albert Sabin Way, Cincinnati, OH 45267-052. Tel.: 513-558-3707; Fax: 513-558-2289; E-mail: Sean.Davidson@UC.edu.

[1] The abbreviations used are: HDL, high density lipoprotein; rHDL, reconstituted HDL; apoA-I, apolipoprotein A-I; PAGE, polyacrylamide gel electrophoresis; POPC, 1-palmitoyl, 2-oleoyl phosphatidylcholine; W@*n*, a single Trp mutant containing Trp at amino acid position *n* with all other sites normally containing Trp converted to Phe; ABCA1, ATP-binding cassette A1; NBD, nitrobenzoxadiazole.

different levels. We found that both Trp residues were maximally quenched at the same level in the bilayer (about 5–6 Å from the bilayer center) as predicted for a belt model (16). This was in direct contrast to synthetic transmembrane peptides in which similarly placed Trp residues were measured in the expected picket fence orientation in vesicles.

In the current study, we report additional control experiments to unambiguously show that helix 4 cannot be in a picket fence orientation by studying additional points along the helix. We then used the same approach to measure the orientation of all remaining 22-amino acid helices in apoA-I. The results show that almost all of the helices orient in some form of a belt-like model. This study identifies the specific regions within the molecule that exist in the belt orientation and lays the foundation for further work aimed at determining the tertiary arrangement of apoA-I molecules on discoidal HDL particles.

EXPERIMENTAL PROCEDURES

Materials

1-palmitoyl, 2-oleoyl phosphatidylcholine (POPC), the nitroxide spin probes 1-palmitoyl, 2-stearoyl(*X*-DOXYL)-*sn*-glycero-3-phosphocholine (where $X = 5$, 7, 10, 12, or 16), and 1-oleoyl, 2-(12-NBD)-*sn*-glycero-3-phosphocholine were purchased from Avanti Polar Lipids (Birmingham, AL). The atomic phosphorus standard was obtained from Sigma. IgA protease was obtained from Mobitec (Marco Island, FL). All other reagents were of the highest quality available.

Methods

Mutagenesis, Protein Expression, and Purification—Human proapoA-I cDNA in the pET30 (Novagen, Madison, WI) vector was used to generate single Trp mutants. Each of the five naturally occurring Trp residues (position −3 in the pro-segment and positions 8, 50, 72, and 108) in proapoA-I were converted to Phe using site-directed mutagenesis (Stratagene, La Jolla, CA), yielding a mutant that contained no Trp residues (W@ϕ). The W@n nomenclature states that a Trp residue has been introduced at position n. We have previously demonstrated that these substitutions do not have major effects on the structure or function of the protein (18). To produce mutants of mature apoA-I that lacked the pro-segment, we added an IgA protease cleavage site to our expression vector between the pro-segment and the beginning of the mature gene.[2] A His tag was included on the extreme N terminus of the construct. Cleavage of the expression product at the IgA protease site removed the pro-segment and His tag, leaving a Thr-Pro on the N terminus of the mature apoA-I protein. W@ϕ was used as a template to insert a Trp residue at a position in the center of an amphipathic helix and, in a separate mutant, at a residue distal to the center of the helix for each of the seven 22-mer helices of apoA-I to be studied (helix 1: W@53,W@60; helix 2: W@75,W@82; helix 5: W@130,W@137; helix 6: W@152,W@159; helix 7: W@174,W@181; and helix 8: W@196,W@203; helix 10: W@229,W@236). Two additional mutants were created in helix 4 at the far N-terminal end (W@101 and W@104) for the described control experiments. Polymerase chain reaction-based site-directed mutagenesis (QuickChange mutagenesis kit; Stratagene, La Jolla, CA) was performed directly in the pET30 expression vector. The sequences were verified on an Applied Biotechnology System DNA sequencer, University of Cincinnati DNA core.

The resulting constructs were transfected into BL-21 (DE3) *Escherichia coli* cells (Novagen). The overexpression of the mutant apoA-I was performed using freshly transfected cells as described previously (18). After harvesting, the cells were resuspended in 10 mM Tris buffer, pH 8.0, containing 0.15 M NaCl, 1 mM EDTA, and 0.2% NaN_3 (standard Tris buffer). The cells were lysed for 20 min at room temperature using B-PER lysis detergent (Pierce) at 4 ml of detergent solution for every 100 ml of bacterial cell culture. The soluble cell contents were applied to a His-bind column (Novagen) and eluted according to the manufacturer's instructions. The His-tagged proteins were dialyzed into 10 mM ammonium bicarbonate buffer, pH 8.0, and lyophilized. Lyophilized proteins were solubilized in 3 M guanidine HCl and dialyzed into standard Tris buffer, and the His tag was then removed by cleavage with 1:5000 (w:w) IgA protease at 37 °C for 16 h. The His tag was removed by hydrophobic interaction chromatography on a phenyl Sepharose HiTrap (Amersham Pharmacia Biotech) column resulting in the final mature apoA-I protein. The proteins prepared by this method were >95% pure as visualized by SDS electrophoresis stained with Coomassie Blue, and the yields were about 3–5 mg of protein/100 ml of original culture.

Preparation and Characterization of the Lipid-containing Particles—rHDL particles were prepared as described previously (20) using POPC, mutant apoA-I, and spin-labeled phospholipids. All phospholipid stock solutions were assayed before the reconstitution by the phosphorus method of Sokolof and Rothblat (21). Initial lipid to protein molar ratios were 85:15:1 (POPC:DOXYL-DSPC:apoA-I) to make 98 Å particles. For each mutant, a set of particles was reconstituted without the spin-labeled phospholipids. Any unreacted protein and vesicular structures were removed by gel filtration chromatography on a Superdex 200 gel filtration column (Amersham Pharmacia Biotech) (22). Previous studies have ensured that the gel filtration step did not change the concentration of quencher within the particles (16). The phosphorus assay and the Markwell modification of the Lowry protein assay (23) determined the final lipid and protein concentrations. Particle hydrodynamic diameters were measured by gradient native polyacrylamide electrophoresis (PhastSystem; Amersham Pharmacia Biotech) (22). The secondary structure content of the apoA-I in the rHDL particles was estimated by circular dichroism at 222 nm (Jasco J-720 spectropolarimeter) (24).

Fluorescence Spectroscopy—All fluorescence measurements were performed on a Photon Technology International Quantamaster spectrometer in photon counting mode. The emission and excitation band passes were 3.0 nm. The excitation wavelength for all Trp studies was 295 nm to minimize the contribution of tyrosine fluorescence in apoA-I. The samples at 0.075 mg/ml in standard Tris buffer for all studies were measured at 25 °C in a semi-micro quartz cuvette. The emission spectra from 305 to 360 nm were corrected for the background fluorescence of buffer alone.

Depth Calculations: Theory—The parallax method for determining the depth of penetration of a fluorophore into a lipid bilayer was derived by Chattopadhyay and London (25) from classical relationships of static quenchers to randomly distributed fluorophores. The method depends on distance-dependent quenching. The differences in fluorescence intensities of the fluorophore in the presence of known concentrations of nitroxide quencher groups at known locations in a phospholipid acyl chain are used to calculate the relative depth of the fluorophore relative to the quenchers (see Ref. 16 for a detailed discussion of the method theory). The distance of the Trp from the center of the bilayer (Z_{cf}) is given by the following equation.

$$Z_{cf} = L_{cs} + [-\ln(F_s/F_d)/\pi C - L_{ds}^2]/2L_{ds} \quad \text{(Eq. 1)}$$

where F_s is the fluorescence intensity in the presence of the shallow quencher, F_d is the same for the deep quencher, L_{cs} is the distance from the center of the bilayer to the shallow quencher, L_{ds} is the distance between the shallow and deep quenchers, and C is the concentration of the quencher molecules/Å^2. Equation 1 holds when the Trp residue is quenched by nitroxide groups shallow in the membrane. When the Trp is buried deep within the membrane, it is subjected to quenching from groups in the opposite side of the lipid bilayer. For this situation, a second relationship is required to account for trans-bilayer quenching.

$$Z_{cf} = L_{cd} - [\ln((F_s/F_o)^2/(F_d/F_o))/\pi C) - 2L_{ds}^2 + 4L_{cd}^2)/4(L_{ds} + L_{cd})] \quad \text{(Eq. 2)}$$

where F_o is the fluorescence intensity in the absence of quencher, L_{cd} is the distance from the center of the bilayer to the deep quencher, and L_{ds} is the distance between the shallow and deep quenchers. Equation 2 was used in this study whenever a Trp residue was determined to be <5 Å from the center of the membrane by Equation 1.

The quenching pair of C-5 and C-12 was chosen for our calculations because these two quenchers gave the largest difference in quenching in previous studies. In addition, Abrams and London (17) have published detailed information on the quenching of 12-NBD phospholipids using the C-5/C-12 pair that allowed the calibration of our particular batches of spin-labeled lipid to estimate Trp depths as accurately as possible (16).

RESULTS

Experimental Design—To determine the orientation of each putative helix of apoA-I, we placed Trp residues at two positions within each helix in separate mutants. ApoA-I has eight generally accepted, 22-amino acid, amphipathic helices (helices 1, 2, 4, 5, 6, 7, 8, and 10). If one assigns the first residue of each helical repeat as position 1 and the last as position 22, then

[2] S. E. Panagotopulos, J. N. Maiorano, E. Horace, and W. S. Davidson, manuscript in preparation.

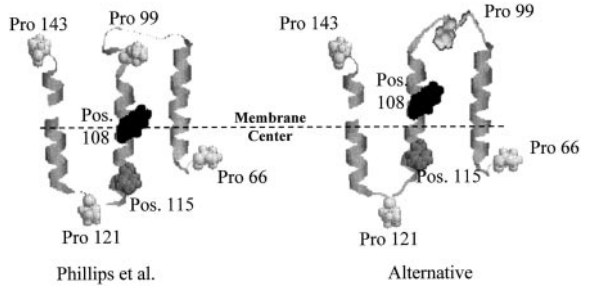

FIG. 1. **Alternative interpretation of Trp depth results for helix 4 of apoA-I.** This figure illustrates that the Trp residues at position 10 and 17 in the 22-mer helical segment could potentially show a quenching pattern consistent with the belt model (both Trp residues quenched at similar levels in the bilayer) but actually be in the picket fence conformation if the helix were shifted 4–5 Å across the bilayer. This has the effect of pulling the central Trp away from its ideal picket fence location near the bilayer center while pulling the distal Trp closer to the center. To rule out this possibility, we performed quenching studies on two additional Trp mutants in which the probe residue was located more N-terminal in the 22-mer helical segment (Fig. 2). The picket fence model shown on the *left* is from Phillips *et al.* (12).

positions 10 and 17 were probed for each helix as in our preliminary study (16). The "central" Trp at position 10 is expected to be about 1.5 Å from the theoretical center of the helix (assuming the center to be 22/2 = 11 and 1.5 Å of distance per residue in an ideal helix). The "distal" Trp at position 17 is two turns along the helix toward the C terminus and theoretically about 9–10 Å from the helix center. These positions have been selected because they are both in the center of the helical hydrophobic face when one looks down the long helical axis and are more than 3 residues away from the extreme ends of the helix. The latter point is important because if there are turn sequences between the helices as predicted by the picket fence model, then both of these positions should be far enough away from the ends so as not to participate in the turns. Thus, we anticipated accurate depth measurements for Trp residues at both positions, regardless of the orientation of the helix with respect to the bilayer.

The Possibility of Helix Sliding—Using this approach, we previously demonstrated that both the central and distal Trp probes in helix 4 of apoA-I were located about 5–6 Å from the center of the bilayer, a result consistent with the belt model. However, the possibility remained that our results could also be consistent with the picket fence model if helix 4 can move upward with respect to the bilayer. This would have the effect of pulling the central Trp away from (and the distal Trp toward) the center of the bilayer with respect to their original positions (Fig. 1). To address this possibility, we constructed two additional mutants that contained Trp residues at positions 3 and 6 in the helical nomenclature (positions 101 and 104 in apoA-I). Although these two residues are close to the N-terminal end of the helix, they are still situated on the hydrophobic face and are 1 and 2 turns N-terminal to the central Trp residue at position 108, respectively (Fig. 2). These two mutants exhibited levels of expression and secondary structure characteristics similar to those of the other mutants created for this particular helix. The fluorescence intensity of each Trp residue in the absence of quencher was compared in the presence of nitroxide-labeled phospholipids in rHDL particles. Fig. 3 demonstrates that both mutants were minimally quenched near the shallow quencher (position C-5) but were increasingly quenched as the nitroxide group was moved deeper into the bilayer. Table I shows that the depth of both Trp residues was about 5–6 Å from the bilayer center, essentially the same position as calculated for the 108 and 115 mutants. The observation of four separate points along the helix at a similar bilayer depth can only be explained by a belt model, assuming that helix 4 is a contiguous helix. With this result established, we generated mutants for the remaining helices in apoA-I at

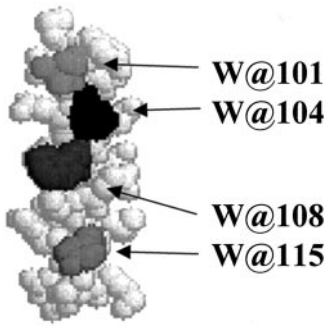

FIG. 2. **Relative positions of the introduced Trp residues within helix 4 of apoA-I.** The isolated helix 4 is taken from the x-ray crystal structure published by Borhani *et al.* (13). Two more N-terminal positions (101 and 104) in addition to the original central and distal Trp residues are highlighted. Notice that all four residues are aligned along the hydrophobic face of the helix.

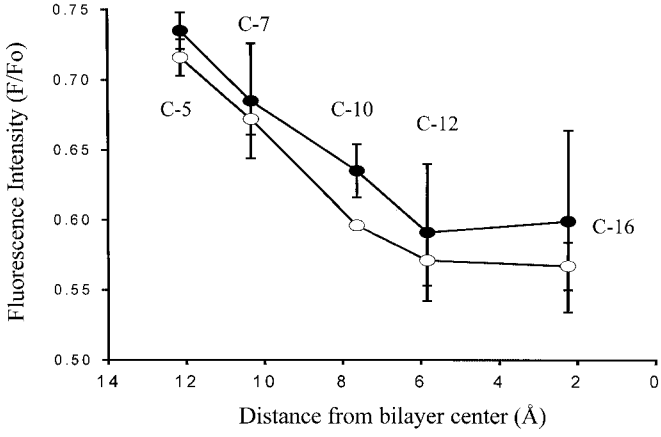

FIG. 3. **Nitroxide lipid quenching pattern for W@101 and W@104 mutants in 98 Å rHDL particles.** The rHDL particles were prepared with each mutant at a molar ratio of 85:15:1 mol:mol:mol (POPC:DOXYL-X PSPC:apoA-I). The 98 Å size classes were purified by gel filtration chromatography, characterized, and used for fluorescence studies at concentrations of 75 μg of apoA-I/ml in standard Tris buffer. The emission spectra were collected from 305–360 nm, and the fluorescence intensity (F) for the DOXYL containing samples at the λ_{max} was plotted as a ratio of the fluorescence of the same particle without quenching groups present (F_o). The excitation wavelength was 295 nm. The labels near each data point indicate the carbon number of the phospholipid acyl chain that contained the quenching group. The X axis shows the distance of each DOXYL group from the center of the membrane (C-5, 12.15 Å; C-7, 10.35 Å, C-10, 7.65 Å; C-12, 5.85 Å, and C-16, 2.25 Å). *Open circles*, W@101; *filled circles*, W@104.

TABLE I
Fluorescence characteristics of Trp mutants generated for helix 4 mutants in 98 Å reconstituted HDL particles

Mutant	Helical position[a]	λ_{max} (± 1 nm)[b]	Z_{cf}[c]
W@101	3	329	5.2 ± 0.7
W@104	6	330	5.3 ± 0.4
W@108	10	327	5.9 ± 0.7
W@115	17	328	6.0 ± 0.9

[a] Position relative to the N-terminal initiating residue of each helix.
[b] The wavelength of maximum fluorescence (λ_{max}) values in this table are average values for all the particles used in analyzing depth for each mutant. For example, the λ_{max} for the W@104 particle was averaged from the particles containing POPC alone, DOXYL-5, and DOXYL-12. We observed no systematic changes in λ_{max} with respect to the presence or position of the nitroxide probe.
[c] The calculated distance from the center of the bilayer to the single Trp residue in each molecule of apoA-I determined from Equations 1 and 2 (see "Methods").

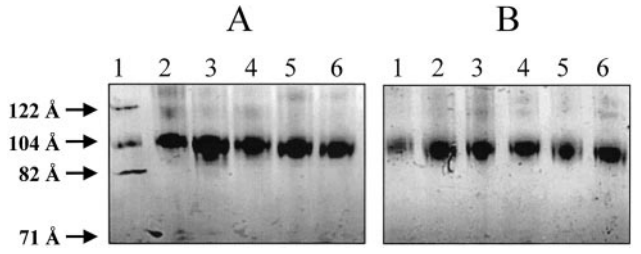

FIG. 4. **Native PAGE analysis of a selection of rHDL particles containing Trp mutants distributed across the entire apoA-I molecule and spin labeled phospholipids at various carbon positions.** Both panels are 8–25% native PAGE gels run side-by-side in the same electrophoresis run on a Phast electrophoresis system stained with Coomassie Blue. 2.4 μg of protein were loaded for each complex. All particles shown were of similar phospholipid to protein molar composition (averaging 96 ± 11:1). All particles exhibited calculated α-helical contents of between 70 and 75% as determined by far UV circular dichroism. *A*, all samples in this panel contain POPC only. *Lane 1*, low molecular weight standards with corresponding hydrodynamic diameters (Amersham Pharmacia Biotech; catalog number 17-0446-01); *lane 2*, human plasma apoA-I rHDL; *lane 3*, W@60 rHDL; *lane 4*, W@82 rHDL; *lane 5*, W@156 rHDL; *lane 6*, W@196 rHDL. *B*, all samples in this panel contained 15 mol % of a nitroxide labeled phospholipid at the indicated carbon position. *Lane 1*, W@130 rHDL (no nitroxide); *lane 2*, W@130 rHDL (nitroxide position 5); *lane 3*, W@130 rHDL (nitroxide position 12); *lane 4*, W@229 rHDL (no nitroxide); *lane 5*, W@229 rHDL (nitroxide position 5); *lane 6*, W@229 rHDL (nitroxide position 12).

helical positions 10 and 17 and measured the relative bilayer depth of each probe.

Generation and Characterization of Mutants in the Other 22-mer Amphipathic Helices of apoA-I—To limit the total number of complexes generated in this study to a reasonable number, we produced three complexes/mutant (one containing no nitroxide, DOXYL-5, and DOXYL-12) rather than using all available nitroxide positions as in our previous studies. These are sufficient for calculation of the depth parameter (17). The initial particle reconstitution reaction conditions were selected to produce primarily 98 Å particles with 90–100 molecules of phospholipid and three molecules of apoA-I/complex. This type of particle was used because of its ease of reconstitution and extreme stability in our hands *versus* those that contain two molecules of apoA-I. Each particle was studied in triplicate from at least two independent preparations of mutant protein. As in our previous study, we expended significant effort to confirm that the introduction of the probe residues did not have adverse effects on the structure of the mutant particles relative to those made with the native protein. We demonstrated that the presence of the nitroxide labels in the rHDL particles did not affect the structure of the associated protein or the size and morphology of the disc (16). Similarly, in the current study, all mutants formed rHDL particles of similar size (about 98 ± 4Å) as measured by native PAGE (Fig. 4) and exhibited similar retention times on a calibrated Superdex 200 gel filtration column (data not shown). A representative selection of these particles is shown in the native PAGE gels in Fig. 4. It is clear that neither the introduction of the Trp residues at various positions across the molecule nor the presence of the spin labels at each position affected the diameter of the particles. This was the case for all the mutants used in this study, even for the relatively poorly conserved substitutions such as Ala residues that were changed to Trp residues. We occasionally saw a slight increase in diameter of rHDL particles generated with human plasma apoA-I *versus* the recombinant form of the protein (on the order of a 2–4 Å). However, this effect is inconsistent between preparations and likely reflected differences in the nature of the protein preparation rather than a significant structural difference between the two types of apoA-I. All particles used were of similar phospholipid to protein molar composition (averaging 96 ± 11:1) to each other and to previously published particles generated with human plasma apoA-I (11, 22), indicating that the Trp mutations do not affect composition of the rHDL particles. Furthermore, the samples selected at random exhibited no significant differences in overall α-helical contents from particles made with wild type protein as determined by far UV circular dichroism (about 70–75% helicity) and were consistent with previous studies of plasma apoA-I particles with this composition. In general, we found that the single Trp substitutions were well tolerated in apoA-I. This result is not surprising because the Trp substitutions were usually quite conservative and only occurred in hydrophobic areas of the molecule that presumably interact with lipid and are not expected to participate in protein-protein interactions in the lipid-bound protein.

TABLE II
Fluorescence characteristics of Trp mutants generated for each putative 22-amino acid amphipathic helix in apoA-I in 98 Å reconstituted HDL particles

Mutant	Helix number and location[a]	λ_{max} (± 1 nm)[b]	Z_{cf} (± 1.0)[c]
W@53	1 (central)	330	**2.4**
W@60	1 (distal)	328	5.4
W@75	2 (central)	327	5.2
W@82	2 (distal)	330	4.0
W@108	4 (central)	327	5.9
W@115	4 (distal)	328	6.0
W@130	5 (central)	327	6.0
W@137	5 (distal)	328	5.4
W@152	6 (central)	328	4.9
W@159	6 (distal)	327	5.5
W@174	7 (central)	330	5.5
W@181	7 (distal)	331	4.2
W@196	8 (central)	**325**	5.0
W@203	8 (distal)	**325**	5.1
W@229	10 (central)	**324**	5.4
W@236	10 (distal)	330	**3.7**
Averages		328 ± 5	5.0 ± 1.0

[a] Helix number is assigned as in Ref. 3. The designation of central or distal refers to helical positions 10 or 17 as numbered from the N-terminal initiating residue of each helix.

[b] Wavelength of maximum fluorescence values in this table were calculated as in Table 1. Bold type has been used for a population of Trp residues that appear to cluster at a more blue-shifted wavelength (near 325 nm) *versus* the majority of the residues that cluster closer to 330 nm.

[c] The calculated distance from the center of the bilayer to the single Trp residue in each molecule of apoA-I determined from Equations 1 and 2 using the −5 and −12 nitroxide positions (see "Methods"). Typical standard deviations from multiple observations are ± 1 Å. Bold type has been used for the two residues that appear to be situated at a deeper position with respect to the bilayer than the majority of other residues based on its value being greater than 1 standard deviation from the mean of all Trp residues.

Table II lists the wavelengths of maximum fluorescence (λ_{max}) measured for each complex. All rHDL particles exhibited blue-shifted λ_{max} values, which are consistent with the Trp residues being involved in lipid contacts (26). Interestingly, the λ_{max} values could be separated into two populations with most of the mutants exhibiting a value of about 330 nm but with three residues in helices 8 and 10 averaging closer to 325. These regions may exhibit particularly tight association with lipid *versus* the other regions. Table II also shows the average depth measurement taken for each probe in each helical region. It is clear that the great majority of the Trp probes were determined to be about 5 Å from the center of the bilayer. The depths of all probes averaged 5.0 ± 1.0 Å. Two exceptions from this pattern were noted based on measured depth values that were more than one standard deviation away from the mean of all samples. The Trps at positions 53 and 236 exhibited values that were slightly closer to the bilayer center than the others.

In the absence of these two samples, the remaining Trp residues averaged to a depth of 5.2 ± 0.6 Å from the bilayer center. There were some other Trp residues that were below the average, but we routinely observe an experimental variation of about 1 Å among similar samples. Thus, we considered differences that are less than 1 Å to be due to experimental variation.

DISCUSSION

The work reported here extends our previous findings by demonstrating that our results for helix 4 were not attributable to movement of the helix across the plane of the bilayer edge in a picket fence model. More importantly, the application of the Trp depth strategy to all putative 22-amino acid repeats demonstrates that the majority of the Trp residues in the helical regions in apoA-I are present at the same level in the bilayer.

The Physiological Significance of apoA-I Helix Orientation in Discoidal Complexes—Discoidal HDL particles do not accumulate to a significant degree in the plasma compartment of normal individuals. Therefore, at first glance, the issue of whether apoA-I encapsulates a discoidal patch of phospholipid in a belt or picket fence orientation may be seen as little more than a trivial geometric problem. However, the recent discovery of the importance of the ABCA1 transporter (27–29) and its possible interaction with lipid-free apoA-I (30) has focused much attention on the phenomenon of apolipoprotein-mediated phospholipid and cholesterol efflux. There is considerable evidence that an ABCA1 controlled pathway is responsible for the initial stages of apoA-I lipidation, especially by phospholipid. By most accounts, the maturation from lipid-free apoA-I to a mature spherical HDL particle likely occurs through some form of discoidal intermediate. This intermediate is short-lived because of the actions of lipoprotein remodeling enzymes such as lecithin:cholesterol acetyl transferase that act quickly to convert nascent particles to more mature forms in plasma, although this may occur more slowly in extravascular compartments where discoidal complexes are measurable (31, 32). In Tangier disease patients, who lack functional ABCA1, there is an almost complete absence of lipidated apoA-I in circulation (33). This strongly suggests that apoA-I is initially secreted in a lipid-free form and requires subsequent lipidation by ABCA1 to avoid premature clearance from circulation. Thus, it can be argued that almost all HDL-associated apoA-I in normal human plasma must have passed through a discoidal intermediate at some point in its circulatory life cycle.

Given the importance of a discoidal intermediate, it follows that the functional predictions derived from the picket fence or belt models have profound physiological implications on apoA-I function and HDL metabolism. Consider the example of a newly formed discoidal HDL particle that contains two molecules of apoA-I. In the picket fence model, a discrete interaction site for lecithin:cholesterol acetyl transferase might be present entirely on each molecule of apoA-I because each molecule forms a distinct face that covers roughly half the circumference of the disc. Conversely, in the double belt model proposed by Segrest *et al.* (14) each molecule stretches all the way around the particle. In this case, it is more likely that the lecithin:cholesterol acetyl transferase activation site on apoA-I is a chimeric region that has elements present on both molecules of apoA-I. A similar case can be made for interactions with cholesterol ester transfer protein, receptors such as SR-B1, or perhaps even the ABCA1 transporter. Therefore, resolution of the structure of disc-bound apoA-I will assist in the identification of these critical interaction regions within apoA-I. This understanding will allow for more informed mutagenesis strategies both *in vitro* and in mouse models to elucidate the molecular details of reverse cholesterol transport.

Models of Apolipoprotein A-I Structure—It is clear from Table II that the Trp residues introduced in helices 2, 4, 5, 6, 7, and 8 closely fit the prediction for a belt model with each Trp between position 60 and 229 averaging about 5.2 Å from the center of the bilayer. We realize that because most of these helices were studied at only two points/helix, one might argue that these helices may still exist in a picket fence orientation in which the helices have slid up and down the bilayer as depicted for helix 4 in Fig. 2. However, a close study of the Phillips picket fence molecular model (12) reveals that to arrange all 16 Trp residues between 60 and 229 at the same depth in the bilayer, one has to accept two major deviations from classical picket fence theory. First, this would require that the helical turns would not be centered on proline residues. Second, it would require the insertion of extended regions of nonhelicity in each putative helix to place the Trp residues in the correct locations. In the absence of evidence for such significant departures from our current understanding of apoA-I structure, we believe that a picket fence organization is highly unlikely given our data and given that expending the resources to study a third point in each helix would be counterproductive.

Interestingly, the central Trp in helix 1 and the distal Trp in helix 10 are the only two that appear to differ from the average depth observed for the other 16 mutants. These two locations are at the extreme ends of the region that we probed in this study. Thus, the locations of both Trp residues in helices 1 and 10 do not strictly fit the predictions of either the picket fence or belt models. An underlying assumption required for distinguishing between the two models in this study is that each helical segment exists as a rigid helical rod. If this assumption holds for helices 1 and 10, then one interpretation would be that both of these helices cross the bilayer at an angle that is intermediate between those predicted for the belt and picket fence models. This is not the first time that helices 1 and 10 have been observed to have distinguishing traits *versus* the internal helices. Palgunachari *et al.* (34) have demonstrated that these same helices exhibit the highest affinity for lipid and may be involved in the initial events of apoA-I lipid binding. Thus, it is possible that the unique orientation parameters that we observed are related to differences in lipid penetration characteristics of these two helices *versus* the others. Alternatively, the assumption of a rigid helical rod may not hold in the case of every single helical segment in apoA-I. Indeed, taking the commonly measured value of about 70–75% helical content for apoA-I in particles of this composition, about 61–73 of the 243 amino acids are predicted to exist in a nonhelical conformation. Even if one assumes that the N-terminal 43 amino acids are predominantly nonhelical (35), there is still significant potential for nonhelicity in the C-terminal 200 amino acids. Thus, we feel that another likely explanation for our observations is that the two end helices may deviate from the expected helical rod and may exhibit an alternative structure (perhaps a random coil or turn motif) near these locations that still allows the Trp residues to interact with lipid. The unusual Trp depth measurement at position 53 may reflect its proximity to the N-terminal 43 amino acids, which have been suggested to exist in a globule-like organization (35). Position 236 is only 7 residues away from the C terminus of the molecule and might also be expected to differ in bilayer position than the central region of the molecule.

The finding that the bulk of the molecule is in a belt-like orientation is highly consistent with two recently reported models of apoA-I. The double belt model of Segrest *et al.* (14) depicts two molecules of apoA-I wrapping around each leaflet in an anti-parallel orientation. In this model, the structure is stabilized by salt bridge interactions that occur intermolecularly between the two molecules. In support of the double belt

model, an analysis of natural mutations of apoA-I showed that very few mutations were observed at the docking interface between the two molecules and that the salt bridge pattern seems to be highly conserved among mammals, birds, and fish (14). These observations imply that an intact docking interface is critical for apoA-I function. In addition, Li *et al.* (36) observed evidence for rhodamine dimers in their recently reported FRET analysis of apoA-I in rHDL. Because both labeled residues are situated in helix 5 (which are predicted to be in close opposition in the double belt model), they interpreted the apparent close approach of these labels to be in support of the double belt.

However, the double belt model is less satisfying when a third molecule is introduced into the disc. Because molecules 1 and 2 occupy both leaflets, molecule 3 must form some sort of a hairpin structure to be accommodated on the disc edge. As of now, there is no definitive data available that justifies such a drastic change in symmetry for the third molecule. A second model initially suggested by Brouillette *et al.* (3) predicts that all molecules on a given particle are arranged in a hairpin orientation. In this model, about half of the molecule is on one leaflet, there is a turn, and the other half precedes anti-parallel to the first on the opposing leaflet. This model is supported by FRET experiments performed by Tricerri *et al.* (19) in which fluorescent acceptor and donor probes were introduced at three positions throughout apoA-I. The distance constraints generated were inconsistent with both the picket fence and double belt models but supportive of the hairpin model in which there was a random distribution of "head-to-tail" and "tail-to-head" orientations. This model is attractive in that it preserves the potential for stabilizing salt bridge interactions between the same residues that were proposed for the double belt model, although these would occur intramolecularly in the hairpin model. In addition, it readily provides for the possibility of three molecules of apoA-I in a discoidal complex in which all three are in a similar conformation. A third model that is also consistent with our data is one that we have termed the "Z" belt model. This arrangement is similar to the hairpin idea except that instead of traversing back along itself, the molecule proceeds in the same direction on the opposing leaflet, giving the potential for interlocking interactions between the molecules. This model also allows for the presence of three molecules on a disc in similar conformations and is the simplest model in terms of symmetry of the apoA-I molecules on the disc edge.

Although our current approach was not capable of distinguishing between these variations of the belt model, our results effectively rule out models that include significant mixtures of the picket fence and belt models. With the knowledge of the regions of apoA-I that are in a belt orientation and the inherent constraints provided by the presence of the protein on the disc edge, the number of possible tertiary models of apoA-I on a disc has been dramatically reduced. In the absence of high resolution structures of the particles from x-ray crystallography or NMR, fluorescence energy transfer approaches appear to be the most promising for distinguishing between the various belt models. The large number of Trp mutants obtained for the current study will be useful in such studies that measure energy transfer from the various single Trp residues to fluorescent acceptor probes attached to introduced cysteine residues at specific locations on other apoA-I molecules on the same disc. Such studies should provide numerous constraints required for deriving a relatively high resolution model of apoA-I structure in discoidal and spherical, HDL particles.

Acknowledgments—We thank Dr. Erwin R. London (State University of New York at Stony Brook) for providing control transmembrane peptides, calibration data and valuable advice and discussion concerning the adaptation of the parallax analysis to reconstituted particles. Finally, we congratulate Dr. Ana Jonas for remarkable scientific and educational accomplishments in the field of lipoprotein structural biology. We wish her the best of luck during her retirement.

REFERENCES

1. Schaefer, E. J., Lamon-Fava, S., Ordovas, J. M., Cohn, S. D., Schaefer, M. M., Castelli, W. P., and Wilson, P. W. (1994) *J. Lipid Res.* **35,** 871–882
2. McLachlan, A. D. (1977) *Nature* **267,** 465–466
3. Brouillette, C. G., and Anantharamaiah, G. M. (1995) *Biochim. Biophys. Acta* **1256,** 103–129
4. Johnson, W. J., Mahlberg, F. H., Rothblat, G. H., and Phillips, M. C. (1991) *Biochim. Biophys. Acta* **1085,** 273–298
5. Glomset, J. A. (1968) *J. Lipid Res.* **9,** 155–167
6. Lawn, R. M., Wade, D. P., Garvin, M. R., Wang, X., Schwartz, K., Porter, J. G., Seilhamer, J. J., Vaughan, A. M., and Oram, J. F. (1999) *J. Clin. Invest.* **104,** R25–R31
7. Acton, S., Rigotti, A., Landschulz, K. T., Xu, S., Hobbs, H. H., and Krieger, M. (1996) *Science* **271,** 518–520
8. Baker, H. N., Gotto, A. M. J., and Jackson, R. L. (1975) *J. Biol. Chem.* **250,** 2725–2738
9. Wald, J. H., Coormaghtigh, E., De Meutter, J., Ruysschaert, J. M., and Jonas, A. (1990) *J. Biol. Chem.* **265,** 20044–20050
10. Brasseur, R., De Meutter, J., Vanloo, B., Goormaghtigh, E., Ruysschaert, J. M., and Rosseneu, M. (1990) *Biochim. Biophys. Acta* **1043,** 245–252
11. Jonas, A., Kezdy, K. E., and Wald, J. H. (1989) *J. Biol. Chem.* **264,** 4818–4824
12. Phillips, J. C., Wriggers, W., Li, Z., Jonas, A., and Schulten, K. (1997) *Biophys. J.*. **73,** 2337–2346
13. Borhani, D. W., Rogers, D. P., Engler, J. A., and Brouillette, C. G. (1997) *Proc. Natl. Acad. Sci. U. S. A.* **94,** 12291–12296
14. Segrest, J. P., Jones, M. K., Klon, A. E., Sheldahl, C. J., Hellinger, M., De Loof, H., and Harvey, S. C. (1999) *J. Biol. Chem.* **274,** 31755–31758
15. Koppaka, V., Silvestro, L., Engler, J. A., Brouillette, C. G., and Axelsen, P. H. (1999) *J. Biol. Chem.* **274,** 14541–14544
16. Maiorano, J. N., and Davidson, W. S. (2000) *J. Biol. Chem.* **275,** 17374–17380
17. Abrams, F. S., and London, E. (1993) *Biochemistry* **32,** 10826–10831
18. Davidson, W. S., Arnvig-McGuire, K., Kennedy, A., Kosman, J., Hazlett, T. L., and Jonas, A. (1999) *Biochemistry* **38,** 14387–14395
19. Tricerri, M. A., Behling Agree, A. K., Sanchez, S. A., Bronski, J., and Jonas, A. (2001) *Biochemistry* **40,** 5065–5074
20. Jonas, A. (1986) *Methods Enzymol.* **128,** 553–582
21. Sokoloff, L., and Rothblat, G. H. (1974) *Proc. Soc. Exp. Biol. Med.* **146,** 1166–1172
22. Davidson, W. S., Rodrigueza, W. V., Lund-Katz, S., Johnson, W. J., Rothblat, G. H., and Phillips, M. C. (1995) *J. Biol. Chem.* **270,** 17106–17113
23. Markwell, M. A., Haas, S. M., Bieber, L. L., and Tolbert, N. E. (1978) *Anal. Biochem.* **87,** 206–210
24. Sparks, D. L., Lund-Katz, S., and Phillips, M. C. (1992) *J. Biol. Chem.* **267,** 25839–25847
25. Chattopadhyay, A., and London, E. (1987) *Biochemistry* **26,** 39–45
26. Burstein, E. A., Vedenkina, N. S., and Ivkova, M. N. (1973) *Photochem. Photobiol.* **18,** 263–279
27. Brooks-Wilson, A., Marcil, M., Clee, S. M., Zhang, L. H., Roomp, K., van Dam, M., Yu, L., Brewer, C., Collins, J. A., Molhuizen, H. O., Loubser, O., Ouelette, B. F., Fichter, K., Ashbourne-Excoffon, K. J., Sensen, C. W., Scherer, S., Mott, S., Denis, M., Martindale, D., Frohlich, J., Morgan, K., Koop, B., Pimstone, S., Kastelein, J. J., and Hayden, M. R. (1999) *Nat. Genet.* **22,** 336–345
28. Bodzioch, M., Orso, E., Klucken, J., Langmann, T., Bottcher, A., Diederich, W., Drobnik, W., Barlage, S., Buchler, C., Porsch-Ozcurumez, M., Kaminski, W. E., Hahmann, H. W., Oette, K., Rothe, G., Aslanidis, C., Lackner, K. J., and Schmitz, G. (1999) *Nat. Genet.* **22,** 347–351
29. Rust, S., Rosier, M., Funke, H., Real, J., Amoura, Z., Piette, J. C., Deleuze, J. F., Brewer, H. B., Duverger, N., Denefle, P., and Assmann, G. (1999) *Nat. Genet.* **22,** 352–355
30. Oram, J. F., Lawn, R. M., Garvin, M. R., and Wade, D. P. (2000) *J. Biol. Chem.* **275,** 34508–34511
31. Wong, L., Curtiss, L. K., Huang, J., Mann, C. J., Maldonado, B., and Roheim, P. S. (1992) *J. Clin. Invest.* **90,** 2370–2375
32. Roheim, P. S., Dory, L., Lefevre, M., and Sloop, C. H. (1990) *Eur. Heart J.* **11,** (Suppl E) 225–229
33. Schaefer, E. J., Zech, L. A., Schwartz, D. E., and Brewer, H. B. (1980) *Ann. Intern. Med.* **93,** 261–266
34. Palgunachari, M. N., Mishra, V. K., Lund-Katz, S., Phillips, M. C., Adeyeye, S. O., Alluri, S., Anantharamaiah, G. M., and Segrest, J. P. (1996) *Arterioscler. Thromb. Vasc. Biol.* **16,** 328–338
35. Nolte, R. T., and Atkinson, D. (1992) *Biophys. J.* **63,** 1221–1239
36. Li, H., Lyles, D. S., Thomas, M. J., Pan, W., and Sorci-Thomas, M. G. (2000) *J. Biol. Chem.* **275,** 37048–37054